Available online at www.sciencedirect.com
SCIENCE DIRECT®
Journal of Power Sources 134 (2004) 222–234
JOURNAL OF POWER SOURCES
www.elsevier.com/locate/jpowsour

DSC investigation of exothermic reactions occurring at elevated temperatures in lithium-ion anodes containing PVDF-based binders

E.P. Roth [a,*], D.H. Doughty [a], J. Franklin [b]

[a] *Lithium Battery R&D Department, Sandia National Laboratories, Albuquerque, NM 87185, USA*
[b] *Solvay Research & Technology, Brussels, Belgium*

Received 8 March 2004; accepted 30 March 2004

Abstract

Differential scanning calorimetry (DSC) has been used to measure the thermal interactions between several binder materials and representative anode carbons both in the presence of cell electrolyte (EC:DEC/1M $LiPF_6$ + 2 wt.% vinylene carbonate) and after washing/drying. Binders consisting of homo- or copolymers of vinylidene fluoride (VDF) were examined as well as other fluorinated and non-fluorinated binder materials. The heat evolved by the reactions of these materials was compared to that arising from other exothermic phenomena occurring in charged anodes at elevated temperatures. A matrix of anode material combinations was designed to investigate the role of carbon structure, carbon surface area, state of charge, binder level and presence of electrolyte. The temperature and magnitude of the exothermic reactions were measured up to 375 °C and average enthalpy values were obtained over several duplicate samples to allow good quantitative comparison of the material reactions. The exothermic anode reactions were sensitive to the state of charge and presence of electrolyte. The magnitude of the reactions increased with increasing surface area of the carbon particles. However, similar reaction enthalpies were seen for all binder materials and binder levels.

Keywords: Li-ion battery; Thermal abuse; DSC; PVDF; Binder; Anode

1. Introduction

The thermal performance and safety of Li-ion cells will have a great impact on future commercial use of these cells in many of the expanding energy storage markets. According to certain studies, the binder material plays a significant role in the exothermic response of these cells under abusive thermal conditions. The purpose of this study was to determine the thermal interactions between several binder materials and lithium intercalated in representative anode carbons in the presence of cell electrolyte. Binders consisting of homo- or copolymers of vinylidene fluoride (VDF) were examined as well as other fluorinated and non-fluorinated binder materials. The heat evolved by the reactions of these materials was compared to that arising from other exothermic phenomena occurring in charged anodes at elevated temperatures. The roles of carbon structure, carbon surface area, state of charge, binder level and presence of electrolyte were investigated using differential scanning calorimetry (DSC). The temperature and magnitude of the exothermic reactions were measured up to 375 °C and comparisons were made between the different material combinations.

2. Survey of binder effects on abuse response of Li-ion batteries

Homo- and copolymers of vinylidene fluoride, collectively referred to here as "PVDF", are commonly used as binders for the electrode active materials of lithium secondary batteries, on account of their desirable properties: processability, electrochemical stability, resistance to electrolytes, flexibility, ability to impart the required cohesion within the electrode coating and its adhesion to the current collectors, etc.

It has however been known for many years that fluoropolymers such as polytetrafluoroethylene can react with metallic lithium [1,2], although PVDF has been shown to be

* Corresponding author. Tel.: +1-505-844-3919; fax: +1-505-544-6972.
E-mail address: eproth@sandia.gov (E.P. Roth).

0378-7753/$ – see front matter © 2004 Elsevier B.V. All rights reserved.
doi:10.1016/j.jpowsour.2004.03.074

much more stable than PTFE in actual lithium-ion battery anodes [3].

A number of experimental studies [4–10], briefly reviewed below, have nevertheless demonstrated that the lithium contained in the charged anodes can react exothermically at elevated temperatures with binders based on PVDF, raising the question of the possible role of PVDF in runaway reactions that may occur when such batteries are subjected to the heating that results from electrical, mechanical or thermal abuse.

Thus, Zhang et al. [4] carried out DSC studies on charged anodes and stated that an exotherm, beginning around 230 °C and peaking towards 300 °C, was probably due to reaction of the PVDF binder with Li.

Lampe-Onnerud et al. [5] concluded, on the basis of DSC studies, that "an exothermic reaction between a PVDF-based binder and a lithiated carbon occurs only at temperatures above 280–320 °C, a temperature high enough to be of little practical concern for small- and moderate-size cells". In further DSC work by the same group [6], it was found that the heat release from the PVDF reaction increased strongly as the degree of lithiation increased, independent of the nature of the carbon; however the reaction occurred only at temperatures higher than 300 °C. The use of a vinylidene fluoride-hexafluoropropylene copolymer [P(VDF-HFP)] was reported to significantly reduce the heat evolved by this reaction, compared to PVDF homopolymer. When polyacrylonitrile or PVC were used as binders, the reaction started at lower temperatures (234 and 270 °C, respectively), but the heat evolved was in the same range as for P(VDF-HFP). It was also observed that the heat generation per unit mass correlated positively with the BET surface area of the anode carbon.

Roth et al. [7], also using DSC, showed that exothermic reactions involving PVDF and intercalated lithium were observed in the 200–300 °C range (with participation of the $LiPF_6$) as well as in the 300–400 °C range. The electrolyte solvent was not directly involved in these reactions.

Biensan et al. [8] reported that the heat evolution observed at temperatures above about 240 °C during DSC tests on charged anodes was considerably greater when PVDF was used as a binder than with unspecified "non-fluorinated binders". Furthermore, it was possible to increase the safe charging voltage of prototype 4/5A cells (as measured using the nail penetration test) by 0.3 V when such a "non-fluorinated binder" was used instead of PVDF.

DSC and ARC studies carried out by Maleki et al. [9] showed that heat generation was significantly lower when the charged anodes were washed in diethyl carbonate to remove electrolyte and then dried, compared to the unwashed anodes. The heat release occurring in washed samples was attributed mainly to the reaction of lithium with PVDF binder. It was confirmed that this reaction begins at around 200 °C and reaches a maximum close to 300 °C. It was also reported that the heat released by a "PVDF-free" negative electrode was significantly lower than that of the same negative electrodes utilizing 8% of PVDF as binder.

In further studies on washed anodes containing 8% PVDF, Maleki et al. [10] showed that heat generation increased steadily with the degree of lithiation. In the case of SFG-44 or MCMB-based anodes, the onset and peak reaction temperatures were around 200 and 300 °C, respectively, independent of the state of charge. When hard carbon was used, onset and peak temperatures were shifted to higher values as the degree of lithiation decreased. Substituting part or all the PVDF by a phenol–formaldehyde binder led to lower heat release.

Richard and Dahn [11] used the ARC technique to study the thermal behavior of lithiated MCMB anodes, made with binders containing PVDF or ethylene–propylene–diene terpolymers. They observed a slightly lower self-heating with the non-fluorinated material, but the maximum temperature studied was only 220 °C, which was most probably too low to observe the full extent of the PVDF–lithium reaction.

In a DSC study carried out by Menachem et al. [12], it was concluded that increasing the PVDF content of an anode from 2.5 to 5% reduced the overall heat release. This may be due to the PVDF partially blocking the pores of the graphite and hence acting as a barrier between intercalated lithium and electrolyte. Analogous observations are reported in the present paper.

Yamaki et al. [13] reported that a DSC exotherm occurred at 140 °C in charged graphite anodes containing PVDF, but was absent in PVDF-free electrodes. They speculated that PVDF, present on the surface of the graphite particles, partially inhibited SEI formation when the electrode was charged at low temperature, but that lithiated areas covered by PVDF were exposed to electrolyte and reacted as the temperature was raised and the PVDF became swollen. They showed that the peak reaction at 280 °C was present even in anodes prepared without any binder, indicating that the binder was only playing a secondary role in the overall anode thermal decomposition.

The possible contribution of PVDF binder to exothermic reactions occurring in lithium battery anodes at elevated temperatures, as reviewed above, needs however to be put into the broader context of the whole range of phenomena leading to heat generation and hence potentially contributing to thermal runaway under abuse conditions. Indeed, there are a number of possible reactions involving other components of the batteries, which may occur at lower temperatures than the reaction of lithium with PVDF:

- solid–electrolyte interphase (SEI) layer decomposition (typically 90–130 °C);
- reaction of intercalated lithium with electrolyte solvent (90–290 °C);
- electrolyte decomposition (200–300 °C);
- positive active material decomposition and reaction with solvent (150–500 °C).

The literature on all these reactions has recently been reviewed by Spotnitz and Franklin [14].

In view of the range of exothermic phenomena that can occur on abuse of a lithium battery, the following questions arise: does PVDF binder in fact contribute significantly to thermal runway? Or, because PVDF reacts with lithium only at relatively high temperatures, is this reaction a consequence rather than a cause of thermal runaway?

Modeling studies intended to resolve this issue were reported recently by Spotnitz and Franklin [14]. The simulations indicate that the PVDF binder plays a relatively unimportant role in thermal runway. Indeed, PVDF has to compete with the solvent for lithium, the latter reaction being more facile and occurring at lower temperatures. So the amount of lithium present is considerably depleted by the time the temperature rises to a level at which the PVDF–lithium reaction could occur. Consequently, reactions involving SEI decomposition, interaction of the intercalated lithium or the cathode material with the solvent and electrolyte decomposition are relatively more important contributors to heat release. Furthermore, runaway reaction is "triggered", following initial ohmic heating resulting from internal or external short-circuit, overcharge, etc., by those reactions which are initiated at the lowest temperatures, namely SEI decomposition and lithium–solvent reaction.

3. Experimental

Electrodes were prepared using combinations of active carbon and binder at both high (10 wt.%) and low (5 wt.%) levels. These binder levels were found to give films with sufficient integrity to result in good capacity levels, cycling stability, and cohesion for subsequent testing. The electrode films were prepared on a copper current collector and then cycled in a T-cell apparatus using Li working and counter electrodes. The electrodes were placed in high (100%) and low (50%) states of charge and then removed in an Ar glove box for DSC analysis. DSC scans were performed on all the electrode compositions in the presence of entrapped electrolyte while some materials were measured after washing/drying to determine the effect of the electrode/electrolyte reactions.

The materials investigated in this study consisted of five different binders and four carbons. The binders included three VDF-based polymers or co-polymers, a polytetrafluoroethylene (PTFE) binder and a non-fluorinated styrene–butadiene rubber/carboxymethylcellulose binder (SBR–CMC). The VDF-based polymers were commercial SOLEF® materials from SOLVAY SOLEXIS. Table 1 lists these binders and their compositions.

The carbon materials consisted of both natural and synthetic graphites with high and low surface areas as determined by BET (Brunauer, Emmett and Teller) analysis. Table 2 lists the carbons and their respective surface areas.

The following matrix shown in Table 3 lists the combination of materials and conditions that were tested. Multiple cells of each material combination were cycled and only cells that showed stable capacities were included for DSC measurements and calculation of average reaction enthalpies.

Table 1
Binder materials

Binder	Composition
SOLEF® 6020	PVDF homopolymer
SOLEF® 21216	P(VDF-HFP): copolymer 88 wt.% VDF, 12 wt.% hexafluoropropylene
SOLEF® 31515	P(VDF-CTFE): copolymer 85 wt.% VDF, 15 wt.% chlorotrifluoroethylene
PTFE	Polytetrafluoroethylene
SBR–CMC	1:1 (w/w) styrene–butadiene rubber/carboxymethylcellulose mixture

Table 2
Anode carbons and their BET surface areas

Carbons	Nominal value (m^2/g)	Measured value (m^2/g)
MCMB 6-28	<4.5	2.5
Timcal SFG 6	17	14.0
Timcal SFG 15	9.5	7.2
Superior Graphite FormulaBT SL 1025	<4.6	4.7

Electrodes were prepared using the doctor blade technique. The VDF-based materials (binder and carbon) were blended in a ball mill for complete mixing and dissolved using DMF. The paste was then spread on copper foil and vacuum baked overnight at 100 °C. This process resulted in films that could be handled and prepared for subsequent electrical cycling without loss of material. The SBR–CMC binders were prepared in aqueous solution in a 1:1 weight ratio and mixed with the carbons to make the electrode paste for doctor blade preparation followed by vacuum/baking. The PTFE binder was mixed with the carbon material using Ligroine solvent (petroleum ether). The thick paste was repeatedly passed through steel rollers until minimum continuous film thickness was obtained and then pressed onto the copper current collector. The films were vacuum/baked as for the other materials. These films tended to be thicker than the doctor blade prepared films.

The electrodes were cycled against Li metal in a half-cell apparatus (T-cell) until a stable capacity was obtained after the initial irreversible losses. Typically three cycles were sufficient to obtain a stable capacity level. The T-cell used 1.5 cm diameter discs cut from the electrode sheets with a Li foil counter electrode and Li reference electrode. The T-cell was prepared in an argon glove box to minimize atmospheric contamination. After placing the electrode materials in the T-cell, the T-cell was evacuated to remove entrapped air and the electrolyte was then introduced through a syringe apparatus. The electrolyte filled the evacuated pores and the whole assembly was allowed to sit overnight to allow the film to fully absorb the electrolyte. The electrolyte consisted of ethylene carbonate/diethyl carbonate (EC/DEC) $1:1\,(v/v) + 1\,M\,LiPF_6 + 2$ wt.% vinylene carbonate (VC).

Table 3
Matrix of electrode materials and measurement conditions

Graphites and binder levels	Binders				
	PVDF homo-polymer, SOLEF® 6020	P(VDF-HFP), SOLEF® 21216	P(VDF-CTFE), SOLEF® 31515	PTFE	SBR–CMC, 1/1 (w/w)
MCMB 6-28	100% SOC in electrolyte	100% SOC in electrolyte			
High (10%)	100% SOC washed/dried	100% SOC washed/dried			
	50% SOC in electrolyte				
Low (5%)	100% SOC in electrolyte	100% SOC in electrolyte	100% SOC in electrolyte	100% SOC in electrolyte	100% SOC in electrolyte
	100% SOC washed/dried	100% SOC washed/dried	100% SOC washed/dried	100% SOC washed/dried	100% SOC washed/dried
	50% SOC in electrolyte	50% SOC in electrolyte	50% SOC in electrolyte	50% SOC in electrolyte	50% SOC in electrolyte
SFG 6	100% SOC in electrolyte	100% SOC in electrolyte			
High (10%)	100% SOC washed/dried	100% SOC washed/dried			
	50% SOC in electrolyte				
Low (5%)	100% SOC in electrolyte	100% SOC in electrolyte			100% SOC in electrolyte
	100% SOC washed/dried	100% SOC washed/dried			100% SOC washed/dried
	50% SOC in electrolyte	50% SOC in electrolyte			50% SOC in electrolyte
SFG 15	100% SOC in electrolyte	100% SOC in electrolyte			
High (10%)	100% SOC washed/dried	100% SOC washed/dried			
	50% SOC in electrolyte				
Low (5%)	100% SOC in electrolyte	100% SOC in electrolyte			100% SOC in electrolyte
	100% SOC washed/dried	100% SOC washed/dried			100% SOC washed/dried
	50% SOC in electrolyte	50% SOC in electrolyte			50% SOC in electrolyte
SL 1025	100% SOC in electrolyte	100% SOC in electrolyte			
High (10%)	100% SOC washed/dried	100% SOC washed/dried			
	50% SOC in electrolyte				
Low (5%)	100% SOC in electrolyte	100% SOC in electrolyte			100% SOC in electrolyte
	100% SOC washed/dried	100% SOC washed/dried			100% SOC washed/dried
	50% SOC in electrolyte	50% SOC in electrolyte			50% SOC in electrolyte

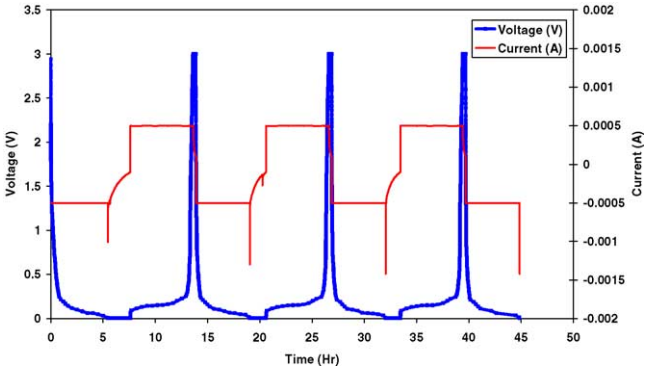

Fig. 1. Electrical cycle profile of typical anode cycled in T-cell.

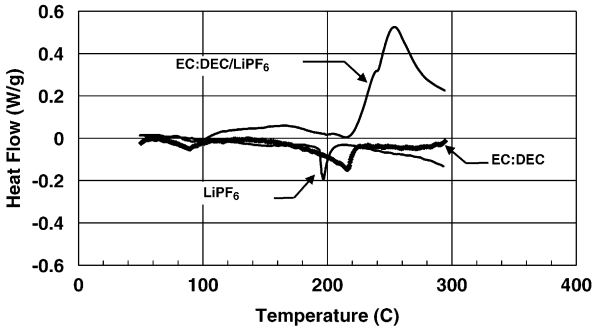

Fig. 2. DSC profiles for EC:DEC/$LiPF_6$ electrolyte, EC:DEC solvent and $LiPF_6$ salt.

Electrical cycling was performed using an Arbin (BT2042) battery cycler with a lithium reference electrode. Charging (lithiation) was performed at 0.5 mA to 4.1 V with a 0.1 mA cutoff. The discharge cycle (delithiation) was also performed at 0.5 mA to 3.0 V with a 0.1 mA cutoff. The maximum current density was 0.28 mA/cm^2. Fig. 1 shows the typical charge/discharge cycles for a total of three cycles. Table 4 lists the average capacity values for the T-cells prepared for DSC measurement at 100% SOC (total of 123 T-cells). The number in parenthesis are the number of cells measured for each material. The standard deviations of the measurements are also listed as a percentage of the average. An additional 24 T-cells were prepared and cycled for the 50% SOC measurements and another 24 T-cells for the washing/drying measurements. The capacity values in Table 4 are given as a percentage of the theoretical limit of 372 mAh/g for intercalating graphites. The MCMB carbons consistently had lower capacity values in the low 80% theoretical range while the other carbons had a 98% theoretical average capacity. The PTFE samples had only a 52% capacity probably resulting from the thicker film and possibly due to poorer particle connectivity.

The cycled anodes were measured in the presence of entrapped electrolyte that typically showed a 1:1 weight ratio between electrolyte and film. Additional measurements were performed on cycled anodes that had been washed with DEC solvent (three times) and dried to remove the salt containing electrolyte. Approximately 85% of the electrolyte was removed by this procedure.

Samples of the electrode materials were cut from the cycled T-cell electrodes for encapsulation in the DSC pans. The T-cells were disassembled and the DSC samples prepared in the Ar glove box. Careful measurements were made of the electrode weights prior to assembly in the T-cell (dry), after removal from the T-cell (wet with electrolyte) and finally after encapsulation in the DSC pans. The amount of electrolyte entrapped in the film pores was determined from these weights and used to limit the total amount of electrolyte included in the DSC pans. Excess electrolyte resulted in pan venting and endothermic thermal signatures. Frequently, the electrode material had to be cut down to limit the amount of sample to be measured. The DSC calculations were based on dry film weight of the electrode material. Care was taken to account for any material lost due to flaking from the electrode during handling and insertion into the DSC pans.

DSC measurements were performed using the TA Instruments model 2910 calorimeter and Thermo-Haake high-pressure DSC pans. These pans are crimped hermetic steel pans that allowed measurement of sample weights up to about 7 mg without venting. DSC scans were performed at a rate of 5 °C/min to a maximum of 375 °C to minimize the possibility of over pressurization. The ratio of entrapped electrolyte weight to film weight was calculated for each sample and showed an overall average of 0.97:1. The sample pan weights were recorded before and after the DSC runs to measure for any mass loss due to venting. As many as one in three steel pans would show weight loss and the data associated with those was not used.

4. Results and discussion

Fig. 2 shows the DSC scans of the starting materials for the electrolyte ($LiPF_6$, EC:DEC) as well as the full electrolyte (EC:DEC, 1 M $LiPF_6$), all measured in hermetic pans. The $LiPF_6$ salt melted at 190 °C while the solvent species (EC:DEC) did not show any exotherms. Mixed together, the $LiPF_6$ salt resulted in an exothermic decomposition of the electrolyte with a peak at 250 °C.

4.1. 100% SOC in electrolyte

Initial measurements were performed on the 22 material combinations at 100% SOC in electrolyte. The enthalpies were calculated by integrating the DSC data from the onset of the exothermic reaction (75 °C) to the completion of the exotherm (300–350 °C) using a linear baseline from the onset to the completion of the reaction region. The reaction enthalpy (J/g) was based on the dry film weight of the sample consisting of the unlithiated carbon and binder. Multiple samples were measured for each material combination and averaged for the final enthalpy value. The enthalpy values for each material varied due to the uncertainties in sample SOC,

Table 4
Average discharge capacities from cycled T-cells for all anode compositions

100% SOC, graphites and binder levels	Binders														
	PVDF homo-polymer, SOLEF® 6020, # cells	mAh/g	%	P(VDF-HFP), SOLEF® 21216, # cells	mAh/g	%	P(VDF-CTFE), SOLEF® 31515, # cells	mAh/g	%	PTFE, # cells	mAh/g	%	SBR–C MC, 1/1 (w/w), # cells	mAh/g	%
MCMB 6-28															
High (10%)	(6)	316.8	83.0	(4)	304	81.3									
	S.D.	5.4%		S.D.	2.1%										
	(5)	306.3	81.6	(6)	291.9	78.5	(3)	307.7	82.7	(7)	197.6	51.8	(5)	290.9	78.2
	S.D.	7.4%		S.D.	9.8%		S.D.	4.2%		S.D.	14.0%		S.D.	4.0%	
SFG 6															
High (10%)	(6)	385.5	102.9	(6)	338.7	95.3									
	S.D.	2.4%		S.D.	11.7%										
Low (5%)	(8)	373.1	100.1	(7)	365.2	98.2							(4)	364.6	98.0
	S.D.	2.4%		S.D.	4.4%								S.D.	2.3%	
SFG 15															
High (10%)	(5)	359	95.3	(6)	383.5	100.3									
	S.D.	4.1%		S.D.	3.7%										
Low (5%)	(7)	360.8	97.2	(7)	377.3	100.6							(5)	365.8	97.8
	S.D.	4.5%		S.D.	2.3%								S.D.	2.2%	
SL 1025															
High (10%)	(6)	378.5	99.6	(8)	358.6	98.0									
	S.D.	4.7%		S.D.	5.0%										
Low (5%)	(9)	367.8	95.5	(9)	350.3	95.5							(6)	352.9	94.9
	S.D.	6.2%		S.D.	7.0%								S.D.	2.9%	

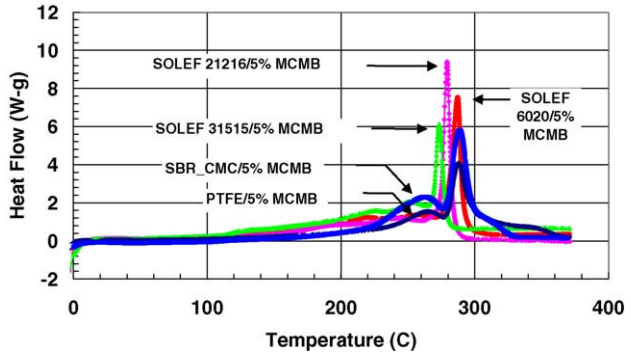

Fig. 3. DSC profiles of all binder materials at the 5% level with MCMB carbon at 100% SOC in electrolyte.

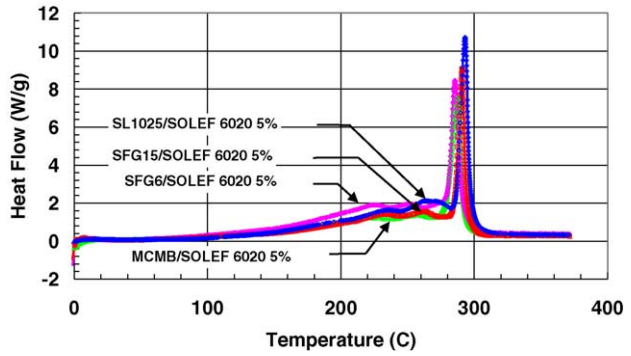

Fig. 4. DSC profiles for all carbons with 5% SOLEF® 6020 binder in electrolyte.

uncertainty in sample weights, variable amounts of DSC pan leakage, and uncertainties in establishing the baseline for the enthalpy calculation. A comparison of the DSC profiles for all the binders at the low 5% level with the MCMB carbon is given in Fig. 3. All measurements were performed at 100% SOC and in the presence of the entrapped electrolyte. The shapes of the DSC curves were quite similar, especially for the VDF-based binders. Low-rate exotherms began as

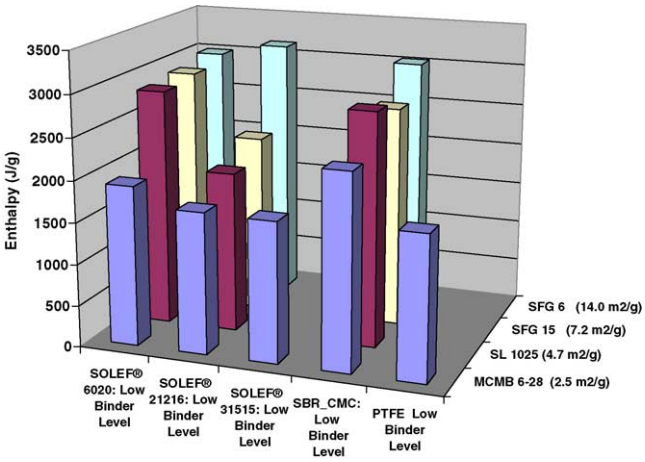

Fig. 5. Average enthalpy values for all materials at 5% low binder level (100% SOC in electrolyte).

low as 50 °C and increased steadily with increasing temperature. The SOLEF® VDF-based polymers showed slightly higher exothermic reaction rates above 100 °C compared to the PTFE and SBR–CMC binders. None of the anode films showed the sharp SEI decomposition exothermic peak often seen in the 100–120 °C range [15,16]. The VC additive may have generated a more stable SEI film that reacted more continuously and slowly with increasing temperature. All the SOLEF® VDF-based binders also showed two lower temperature peaks near 225 and 255 °C. Only a single reaction peak around 260 °C was seen for the PTFE and SBR–CMC binders in this range. This peak corresponds to the peak seen in Fig. 2 for the EC:DEC electrolyte and may have resulted from decomposition of excess electrolyte. Final exothermic reactions occurred with high-rate peaks between 275 and 290 °C.

A comparison of the DSC profiles for all the carbon materials with 5% SOLEF® 6020 binder is shown in Fig. 4. The carbon materials all behaved very similarly showing the gradual increase in heat output with increasing temperature

Table 5
Average DSC enthalpy values for anode compositions at 100% SOC in electrolyte

Graphites and binder levels	Binder enthalpy (J/g)				
	PVDF homo-polymer, SOLEF® 6020	P(VDF-HFP), SOLEF® 21216	P(VDF-CTFE), SOLEF® 31515	SBR–CMC	PTFE
MCMB 6-28					
High (10%)	(3) 1738	(2) 2040			
Low (5%)	(2) 1923	(2) 1699	(3) 1685	(4) 2337	(5) 1727
SL 1025					
High (10%)	(4) 1797	(3) 2457			
Low (5%)	(2) 2850	(3) 1929		(3) 2812	
SFG 15					
High (10%)	(3) 2661	(3) 2646			
Low (5%)	(3) 2901	(3) 2151		(4) 2655	
SFG-6					
High (10%)	(3) 2733	(2) 2746			
Low (5%)	(2) 2996	(2) 3146		(4) 3032	

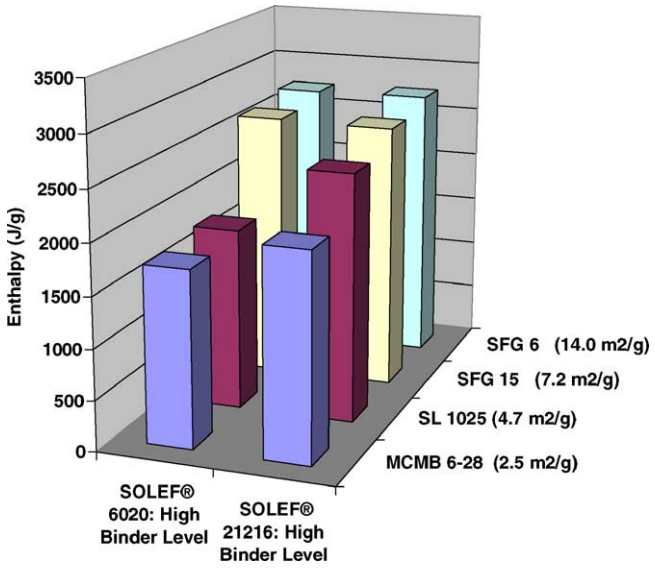

Fig. 6. Comparison of average enthalpy values for binder materials SOLEF® 6020 and SOLEF® 21216 (10% high binder level, 100% SOC in electrolyte).

followed by the two moderate peaks between 220 and 265 °C and finally a high-rate peak between 285 and 295 °C.

Table 5 lists the average total enthalpy values over the whole temperature range for these materials at 100% SOC. The number of cells included in each average are indicated in parentheses. The average standard deviation of all the enthalpy calculations was 17%. Fig. 5 shows a bar chart comparison of the enthalpy data for the low binder level materials. The lowest enthalpies occurred for the lowest surface area carbon (MCMB) and generally increased with increasing surface area. The highest surface area carbon (SFG 6) had the highest enthalpy values. The consistently low values for the MCMB carbons may also be partially due to the lower capacity values for this carbon. The high binder level materials (SOLEF® 6020 and SOLEF® 21216) are shown in Fig. 6. Again, reaction enthalpies increased with increasing surface area. Figs. 7 and 8 compare the high and

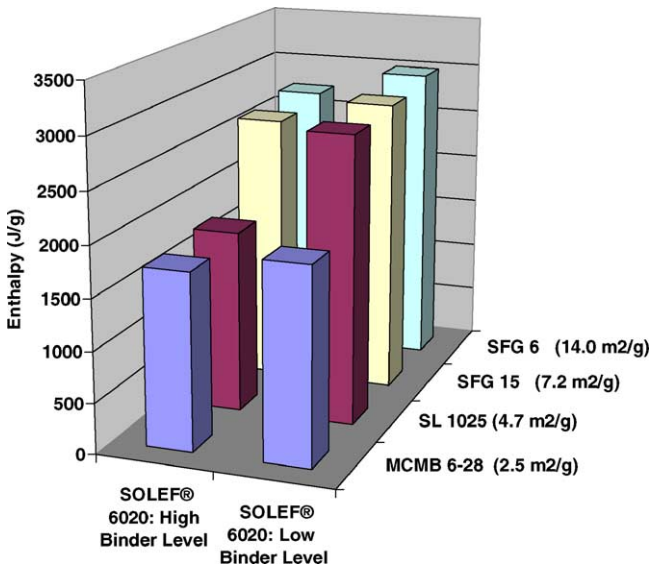

Fig. 7. Comparison of enthalpies for 10% high and 5% low binder levels for SOLEF® 6020 homopolymer.

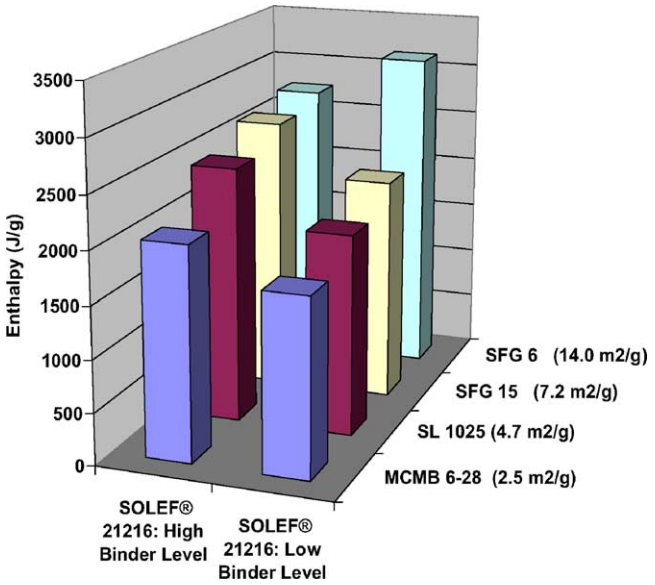

Fig. 8. Comparison of enthalpies for 10% high and 5% low binder levels for SOLEF® 21216 co-polymer.

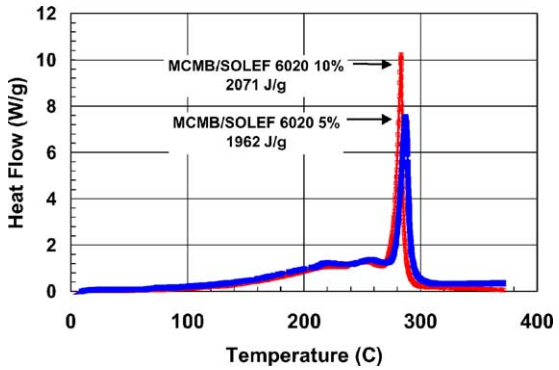

Fig. 9. DSC profile for MCMB carbon with high and low levels of SOLEF® 6020 binder.

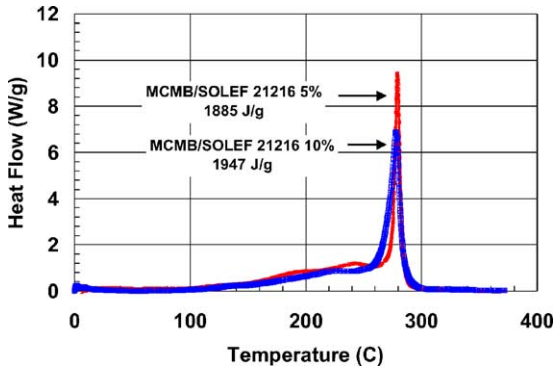

Fig. 10. DSC profile for MCMB carbon with high and low levels of SOLEF® 21216 binder.

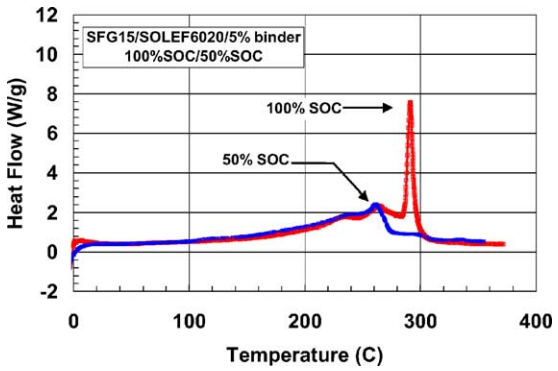

Fig. 11. DSC comparison runs of low binder level material at 50 and 100% SOC.

low binder levels for SOLEF® 6020 and SOLEF® 21216, respectively. The low binder material for SOLEF® 6020 had slightly higher enthalpies while the low binder materials for SOLEF® 21216 had lower enthalpies. Figs. 9 and 10 show the DSC traces for these two binders with the MCMB carbon. No significant difference was seen in these exothermic profiles as a function of binder level for either binder.

4.2. 50% SOC in electrolyte

A total of 18 selected material combinations were also measured at 50% SOC in electrolyte and compared to the 100% SOC measurements. All anode coatings made with the four carbons and SOLEF® 6020 were measured at both high and low binder levels. The SOLEF® 21216 and SBR–CMC binders were measured for all carbons only at the low binder level. Finally, SOLEF® 31515 and PTFE binders were measured only for the MCMB carbon at the low binder level. The electrodes were placed at the desired SOC by first measuring the capacity during the 100% SOC cycles for each T-cell and then coulometrically removing 50% of the measured capacity. The DSC profile for the 50% SOC material typically showed a loss of the high temperature exotherm at 280 °C as illustrated in Fig. 11. The loss of the high temperature exotherm may result from the lack of Li in the anode at those elevated temperatures. The initial low level of Li is being further consumed during the DSC scan at lower temperatures by reaction with the electrolyte after the decomposition of the SEI layer around 120 °C.

The 50% SOC reaction enthalpies were calculated as for the 100% SOC materials and are summarized in Table 6. The values in parenthesis indicate the number of measurements used in each average. Fig. 12 shows a bar chart of the enthalpies for the low binder level materials. As for the 100% SOC materials, the lowest surface area carbon (MCMB) had the lowest average enthalpies while the other higher surface area carbons all had similar average enthalpy values. The ratios of the enthalpies measured at 50 and 100% SOC are given in Table 7. No systematic trend was seen in these ratios indicating the low binder level material combinations all reacted similarly to a reduction in the lithiation level. The overall enthalpy ratio of the 50–100% SOC materials was 0.62:1 with a 13.5% standard deviation.

One binder (SOLEF® 6020) at the low binder level was also measured at 50% SOC. Fig. 13 compares the enthalpies of the 50 and 100% SOC materials with this binder and the different carbons. Table 8 lists the ratio values for each carbon at this high binder level along with the ratios for the low binder level carbons already given. The carbons with this high binder level had an overall average enthalpy ratio of 0.48:1 with a 15% standard deviation compared to a ratio of 0.58:1 at the low levels of this binder. Again, no systematic trend in the reaction enthalpies was seen for the carbon materials at the high binder level.

4.3. Electrode materials without electrolyte (washed/dried)

Materials at 100% SOC were measured without the presence of electrolyte after a washing/drying procedure. The same material combinations (22) were measured as for the

Table 6
Reaction enthalpies for all material combinations at 50% SOC in electrolyte

Graphites and binder levels	Binder enthalpies (J/g)				
	SOLEF® 6020	P(VDF-HFP), SOLEF® 21216	P(VDF-CTFE), SOLEF® 31515	SBR–CMC	PTFE
MCMB 6-28					
High (10%)	(4) 742				
Low (5%)	(4) 1391	(6) 1064	(3) 1376	(6) 1023	(5) 1171
SFG 6					
High (10%)	(4) 845				
Low (5%)	(4) 1870	(2) 1583		(2) 1694	
SFG 15					
High (10%)	(3) 1425				
Low (5%)	(5) 1292	(3) 1557		(3) 1792	
SL-1025					
High (10%)	(3) 1169				
Low (5%)	(6) 1508	(2) 1628		(3) 1831	

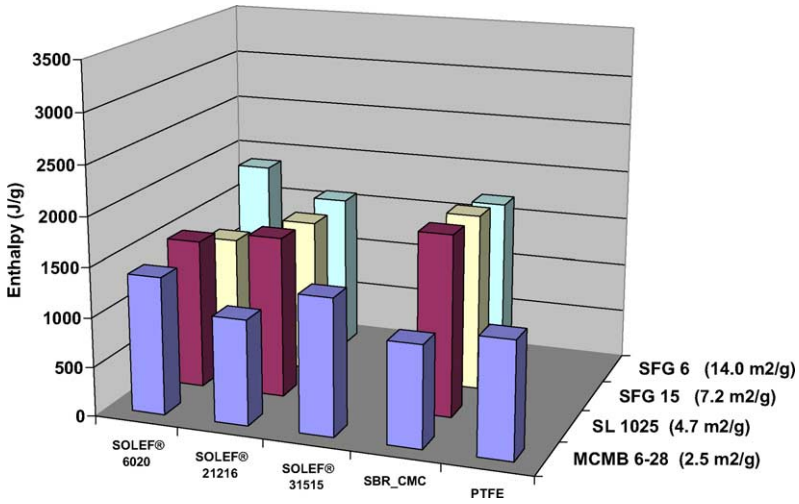

Fig. 12. Average enthalpy values for all materials at the 5% low binder level (50% SOC in electrolyte).

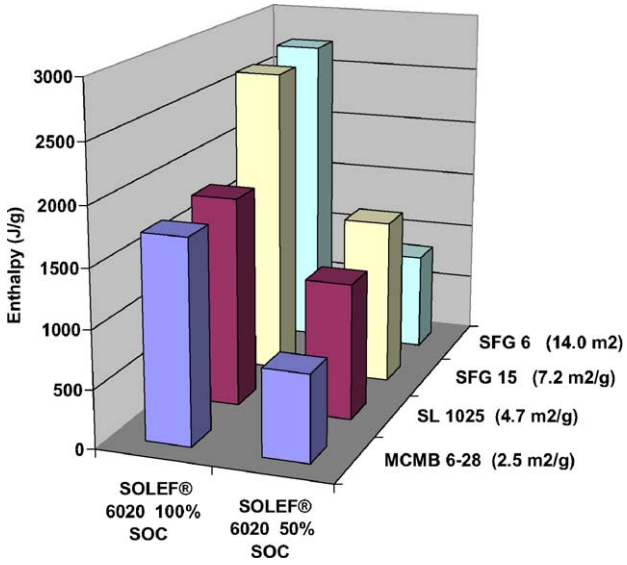

Fig. 13. Average enthalpy values for the 10% binder level SOLEF® 6020 at 50 and 100% SOC.

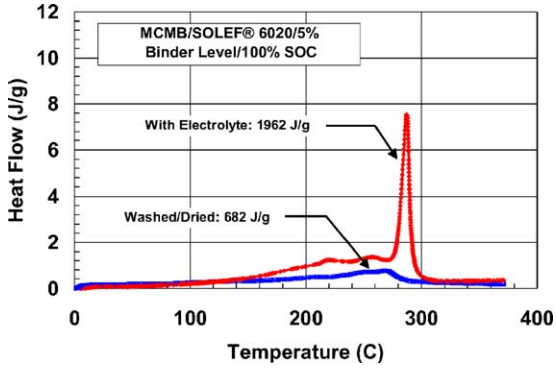

Fig. 14. DSC profile of MCMB/SOLEF® 6020/low binder/100% SOC with electrolyte and after washing/drying.

100% SOC samples in electrolyte but only one sample of each combination was measured. The washing/drying procedure used DEC solvent to rinse the samples (three times) followed by vacuum drying overnight. Typically, 10–15% of the electrolyte remained in the film. Much longer drying periods would be necessary to remove more of the electrolyte. The DSC runs of these materials were performed using the steel crimped pans as described earlier. The DSC traces were less distinct than the runs with the electrolyte, usually showing greatly reduced exothermic reactions at all temperatures and a loss of the peak exotherm at 280 °C. Figs. 14 and 15 show typical DSC traces (MCMB/SOLEF® 6020) at low

Table 7
Enthalpy ratios for 5% low binder level materials at 50 and 100% SOC

	Low binder levels ratios, 50% SOC/100% SOC						
	SOLEF® 6020	SOLEF® 21216	SOLEF® 31515	SBR–CMC	PTFE	Average of binders:	S.D.
MCMB 6-28 (2.5 m^2/g)	0.72	0.63	0.89	0.44	0.68	0.67	0.16
SL 1025 (4.7 m^2/g)	0.53	0.84		0.65		0.67	0.16
SFG 15 (7.2 m^2/g)	0.45	0.72		0.67		0.61	0.15
SFG 6 (14.0 m^2/g)	0.62	0.50		0.56		0.56	0.06
Average of carbons	0.58	0.67	0.89	0.58	0.68		
S.D.	0.12	0.14		0.11			
Total average ratio	0.62						
S.D.	0.14						

Table 8
Enthalpy ratios for 10% high binder level SOLEF® 6020 at 50 and 100% SOC

	High binder levels ratios, 50% SOC/100% SOC	
	SOLEF® 6020: high binder level	SOLEF® 6020: low binder level
MCMB 6-28 (2.5 m^2/g)	0.43	0.72
SL 1025 (4.7 m^2/g)	0.65	0.53
SFG 15 (7.2 m^2/g)	0.54	0.45
SFG 6 (14.0 m^2/g)	0.31	0.62
Average ratio	0.48	0.58
S.D.	0.15	0.12

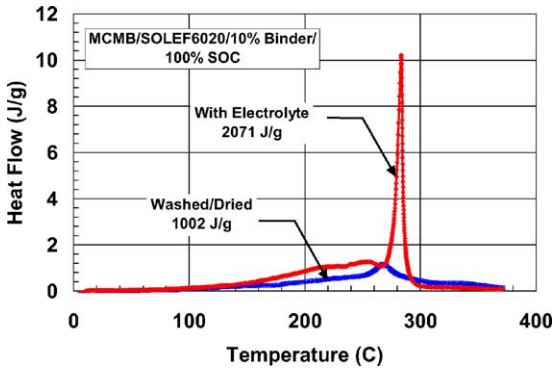

Fig. 15. DSC profile of MCMB/SOLEF® 6020/high binder/100% SOC with electrolyte and after washing/drying.

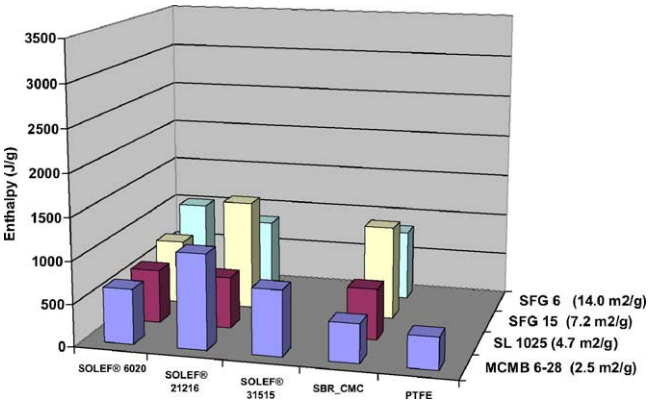

Fig. 16. Enthalpies for low binder level materials at 100% SOC after washing/drying.

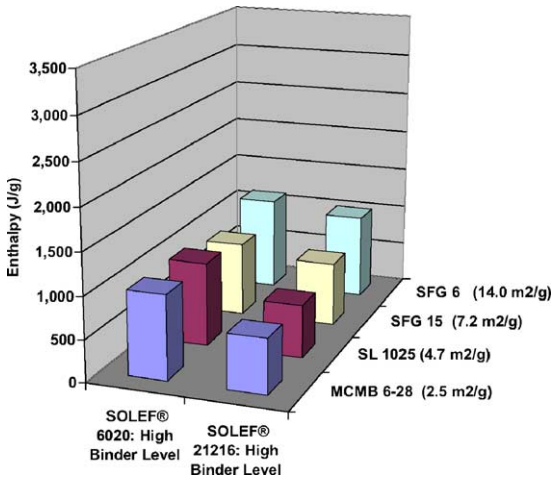

Fig. 17. Enthalpies for high binder level materials at 100% SOC after washing/drying.

and high binder level, respectively, illustrating this behavior. Table 9 lists the reaction enthalpies for all these materials while Figs. 16 and 17 show the bar graphs of the low and high binder level data. Table 10 lists the ratios of enthalpies for the washed/dried anodes to the anodes in electrolyte. Removal of the majority of the electrolyte resulted in a 34–81% reduction in the reaction enthalpies. The VDF-based binders showed an average ratio of 0.42:1 (58% enthalpy reduction) while the non-VDF-based binders showed a ratio of 0.25:1 (75% reduction). The VDF-based binders may have resulted in greater retention of the electrolyte in the anode pores or absorbed into the binder itself resulting in greater residual

Table 9
Average enthalpies of washed/dried anodes at 100% SOC

Graphites and binder levels	Binder enthalpies (J/g)				
	PVDF homo-polymer, SOLEF® 6020	P(VDF-HFP), SOLEF® 21216	P(VDF-CTFE), SOLEF® 31515	SBR–CMC, 1/1 (w/w)	PTFE
MCMB 6-28					
High (10%)	1002	867			
Low (5%)	649	1119	770	455	378
SL 1025					
High (10%)	664	1013			
Low (5%)	633	611		600	
SFG 15					
High (10%)	887	1149			
Low (5%)	765	1297		1108	
SFG-6					
High (10%)	1126	1074			
Low (5%)	1019	855		840	

Table 10
Enthalpy ratios of washed/dried anodes to anodes in electrolyte

100% SOC, graphites and binder levels	Binder enthalpy ratios of washed/dried to electrolyte				
	PVDF homo-polymer, SOLEF® 6020	P(VDF-HFP), SOLEF® 21216	P(VDF-CTFE), SOLEF® 31515	SBR–CMC, 1/1 (w/w)	PTFE
MCMB 6-28					
High (10%)	0.58	0.43			
Low (5%)	0.34	0.66	0.46	0.19	0.22
SL 1025					
High (10%)	0.56	0.41			
Low (5%)	0.22	0.32		0.21	
SFG 15					
High (10%)	0.33	0.43			
Low (5%)	0.26	0.60		0.42	
SFG-6					
High (10%)	0.41	0.39			
Low (5%)	0.34	0.27		0.28	
High average	0.47	0.42			
Low average	0.29	0.46	0.46	0.28	0.22

reaction with lithiated carbon. The loss of the 280 °C peak after washing/drying indicates that the peak reaction is not a direct reaction between the carbon and the binder material.

5. Conclusions

The exothermic reactions of anode films have been measured by DSC for a variety of carbons with increasing surface area and a variety of binder materials including fluorinated and non-fluorinated species. The enthalpies of reaction have been measured carefully with respect to the dry film weight under varying conditions of state of charge and binder level. The DSC measurements were carried out on the films in the presence of the absorbed electrolyte and also after removal of most the electrolyte by a washing/drying process.

The DSC exotherm profiles were similar for all materials and showed the exothermic behavior seen for many similar material systems. Exothermic reactions at the anode in the presence of electrolyte initiate by the breakdown of the protective SEI layer which allows the lithiated carbon to reduce the electrolyte and form additional SEI products. This reaction begins around 120 °C with the decomposition of the SEI layer formed during initial electrical cycling. The high temperature reaction products do not form an effective protective layer at these temperatures and the reaction between the lithiated carbon and the electrolyte continues with increasing temperature. A peak around 280 °C results from the final decomposition of the SEI layer. These anodes were prepared using the VC additive and few of the anode materials showed the peak in the SEI decomposition reaction around 120 °C that we usually observe for materials prepared in the VC-free electrolyte. The VC apparently results in a more robust SEI layer that decomposes more gradually with increasing temperature.

The magnitude of the reaction enthalpies was generally seen to increase with increasing surface area of the carbons with the MCMB carbons having the least enthalpies and the SFG 6 having the greatest. The consistently low values for the MCMB carbons may also be partially due to the lower capacity values for this carbon. The reaction enthalpies for the different binders were very similar for the same measurement conditions. No significant difference was seen due to differences in polymers formed from just the VDF monomer or with co-polymers. No significant difference was seen between the fluorinated binders and the non-fluorinated binders. This result indicates that binder reactions are probably not contributing significantly to the overall exothermic decomposition of the film. Binder reactions may conceivably contribute at temperatures greater than 375 °C (not examined in this study), if indeed any lithium remains unreacted when these temperatures are reached. In any case, such reactions would not play a role in the onset of thermal runaway or in the main exothermic reactions which occur at the point of rapid thermal decomposition and cell disassembly (around 200 °C).

Graphites were tested with both high and low binder levels, but there was no clear correlation between binder content and heat evolved. The variations in reaction enthalpies were much less than the difference in binder levels (a factor of 2) again indicating that the binders are not a direct contributor to the overall exothermic reactions. The binders may have a secondary role in these reactions by affecting the available surface area of the lithiated carbons that can react with the electrolyte. If the binder serves as an effective layer to block the electrolyte at the carbon surface, increased binder level could reduce the reaction rate. However, we did not see a consistent trend between the high and low binder level materials either from the magnitude of the exotherms or the DSC profiles. Binder level has a

minimal effect on the thermal response of the anode reactions.

State of charge had a very strong impact on the exothermic anode reactions. Reduction of the state of charge from 100 to 50% resulted in a 40–50% reduction in the total reaction enthalpies. Most noticeable was the loss of the exothermic peak at 280 °C. The loss of the high temperature reaction peak may result from the lack of Li in the anode at those temperatures. The Li is being consumed during the DSC scans at lower temperatures by reaction with the electrolyte after the decomposition of the protective anode SEI layer. Thus, Li is an essential reactant in these exothermic reactions.

The electrolyte played an essential role in the decomposition reactions. These anode films were observed to entrap electrolyte at a weight level equal to that of the film itself. Washing/drying the films to remove the entrapped electrolyte reduced the electrolyte level by about 85% by weight. The resultant DSC profiles showed a reduced reaction rate at all temperatures but most noticeable was the loss of the 280 °C exotherm. Removal of the electrolyte resulted in a 35–80% reduction of the reaction enthalpies.

We have shown that Li and electrolyte are important reactants in anode thermal decomposition while the binder composition and binder level do not significantly affect the heat evolved. However, we have shown that the enthalpy of reaction increases with increasing carbon surface area. We have determined quantitative values for these reactions over a range of carbon and binder materials based on the dry film weights. Our general observations are that the VDF-based binders, as well as the other binders, incorporated into the anode films do not contribute to the thermal runaway reactions in Li-ion cells.

Acknowledgements

This study was carried out with funding from Solvay Research & Technology, Brussels, Belgium. Thanks also to Dr. Philippe Biensan of SAFT for providing the samples of SBR and CMC binder material.

Sandia is a multiprogram laboratory operated by Sandia Corporation, a Lockheed Martin Company,for the United States Department of Energy's National Nuclear Security Administration under contract DE-AC04-94AL85000.

References

[1] J. Jansta, F.P. Dousek, Electrochim. Acta 18 (1973) 673–674.
[2] J. Jansta, F.P. Dousek, Carbon 18 (1980) 433–437.
[3] W. Liu, X. Huang, G. Li, Z. Wang, H. Huang, Z. Lu, R. Xue, L. Chen, J. Power Sources 68 (1997) 344–347.
[4] Z. Zhang, D. Fouchard, J.R. Rea, J. Power Sources 70 (1998) 16–20.
[5] C. Lampe-Onnerud, D. Culver, A. Du Pasquier, J.A. Shelburne, I. Plitz, A.S. Gozdz, P.C. Warren, J.-M. Tarascon, Recent advances in Bellcore's PLiON™ battery technology—some safety aspects, in: Proceedings of the 15th International Seminar and Exhibit on Primary and Secondary Batteries, Fort Lauderdale, FL, USA, March 2–5, 1998.
[6] A. Du Pasquier, F. Disma, T. Bowmer, A.S. Gozdz, G. Amatucci, J.-M. Tarascon, J. Electrochem. Soc. 145 (2) (1998) 472–477.
[7] E.P. Roth, G. Nagasubramanian, D.R. Tallant, M. Garcia, SANDIA Report SAND99-1164, available from NTIS, US Department of Commerce, Springfield, VA, 1999.
[8] Ph. Biensan, B. Simon, J.P. Peres, A. de Guibert, M. Broussely, J.M. Bodet, F. Perton, J. Power Sources 81–82 (1999) 906–912.
[9] H. Maleki, G. Deng, A. Anani, J. Howard, J. Electrochem. Soc. 146 (9) (1999) 3224–3229.
[10] H. Maleki, G. Deng, I. Kerzhner-Haller, A. Anani, J.N. Howard, J. Electrochem. Soc. 147 (12) (2000) 4470–4475.
[11] M.N. Richard, J.R. Dahn, J. Power Sources 83 (1999) 71–74.
[12] C. Menachem, D. Golodnitsky, E. Peled, Safety issues in lithium-ion rechargeable batteries: anode–electrolyte thermal reactions, in: Abstracts of the Ninth International Meeting on Lithium Batteries, Edinburgh, July 12–17, 1998, p. 74.
[13] J.-I. Yamaki, H. Takatsuji, T. Kawamura, M. Egashira, Solid State Ion. 148 (2002) 241–245.
[14] R. Spotnitz, J. Franklin, J. Power Sources 113 (2003) 81–100.
[15] M.N. Richard, J.R. Dahn, J. Electrochem. Soc. 146 (1999) 2068–2077.
[16] M.N. Richard, J.R. Dahn, J. Electrochem. Soc. 146 (1999) 2078–2084.